Available online at www.sciencedirect.com
ScienceDirect
Journal of Nuclear Materials 362 (2007) 343–349
journal of nuclear materials
www.elsevier.com/locate/jnucmat

Structural investigation on an aged americium transmutation fuel

M. Walter [a,*], J. Somers [a], A. Fernandez [a], D. Haas [a], K. Dardenne [b], M.A. Denecke [b]

[a] European Commission, Joint Research Centre, Institute for Transuranium Elements, P.O. Box 2340, D-76125 Karlsruhe, Germany
[b] Forschungszentrum Karlsruhe, Institut für Nukleare Entsorgung (INE), P.O. Box 3640, D-76021 Karlsruhe, Germany

Abstract

Within the EFTTRA-T4 project a $MgAl_2O_4$ based inert matrix fuel for ^{241}Am transmutation was produced in 1996. Am L_3-edge EXAFS of the annealed material indicate that Am is present as $AmAlO_3$. During 10 years of storage the material accumulated self-irradiation damage and no $AmAlO_3$ X-ray diffraction features can be observed, indicating amorphization of the aged material by the corresponding cumulative α-damage of 2.9×10^{19} g^{-1} $AmAlO_3$. The Am L_3-edge EXAFS of the amorphous $AmAlO_3$ shows that structural order is limited to the first oxygen shell around Am, where the rhombohedral splitting in three sub-shells is still present. Evidence for a single Al atom in the next shell is found at an Am–Al distance of 3.28 Å.

PACS: 507

1. Introduction

The transmutation of minor actinides (MA: Np, Am, Cm) in fast reactors or accelerator driven systems is a recent innovative approach to reduce their long-term radiotoxicity. To obtain a high MA burn up, inert matrices are necessary as host matrices for the minor actinides [1]. Due to its advantageous physical properties (high melting point, resistance to damage), spinel ($MgAl_2O_4$) was chosen as such an inert matrix for the EFTTRA (experimental feasibility of targets for transmutation) T4 experiment [2]. In this experiment, porous spinel pellets were infiltrated with about 11 wt% ^{241}Am [3] and then sintered at 1873 K. As indicated by optical microscopy of polished sections, Am forms a dispersed separate phase in the spinel matrix with a particle size of less than 3 μm. The structure of the Am-bearing phase was not clear, however, and a perovskite-like phase $AmAlO_3$ appeared to form during sintering [2,3]. This material was irradiated at the High Flux Reactor Petten from 1996 to 1998 (T4) and 1997 to 1999 (T4bis) and the results of post-irradiation examination are reported elsewhere [3–5]. Since preparation (June 1996), the stored un-irradiated archive material underwent radiation damage due to α-decay of ^{241}Am. Since then 1.4% of the initial ^{241}Am has decayed to ^{237}Np, resulting

* Corresponding author. Tel.: +49 7247 951 130; fax: +49 7247 951 566.
E-mail address: marcus.walter@ec.europa.eu (M. Walter).

0022-3115/$ - see front matter © 2007 Elsevier B.V. All rights reserved.
doi:10.1016/j.jnucmat.2007.01.082

in a cumulative α-damage of 4.3×10^{18} g^{-1} for the bulk matrix. Considering that the Am is concentrated in a separate phase and that short ranging recoil nuclei dominate the amorphization process [6], the cumulative α-dose is 2.9×10^{19} g^{-1} in the Am containing phase.

In contrast to the rare-earth homologues, the crystallographic structure of the transuranium aluminates is not well known. In the rare-earth aluminates, $LaAlO_3$ has the lowest distortion from the ideal cubic perovskite structure, the rhombohedral $R\bar{3}c$ structure. Distortion increases within the lanthanide series and from $SmAlO_3$ to $LuAlO_3$ the less symmetric orthorhombic structure *Pbnm* is stable at room temperature [7,8]. $PuAlO_3$, $AmAlO_3$, $CmAlO_3$ crystallize in the rhombohedral space group $R\bar{3}c$ [9–11]. The $AmAlO_3$ lattice parameters were reported as $a = 5.336$ (5) and $c = 12.91$ (2) Å, but no information about the atomic positions are available [10]. However, the lattice parameters are nearly identical with those of $NdAlO_3$, for which the atomic positions are known [12,13]. With increasing temperature the lattice relaxes and distortion decreases. As indicated by neutron diffraction, $LaAlO_3$ becomes cubic above 820 K, whereas the rhombohedral to cubic transition temperature of $NdAlO_3$ seems to be higher than 1673 K [13]. For $CmAlO_3$ this transition is reported below 773 K [11]. Mosley [11] also indicated that self-irradiation damage swells the $^{244}CmAlO_3$ lattice, which stabilizes the cubic structure at room temperature before it becomes amorphous.

The swelling induced by accumulation of self-irradiation can be monitored by the change in unit cell dimensions or macroscopically by the change in material density. At higher doses many materials become amorphous, which limits the application of X-ray diffraction techniques. Extended X-ray absorption fine structure (EXAFS) is well suited for the provision of information on the local metal environment in such amorphous materials [14]. EXAFS studies of metamict natural minerals [15] and ^{238}Pu doped waste forms such as zirconolite [16] and zircon [17] show a loss of long range order with accumulation of self-irradiation, whereas the nearest-neighbour coordination shell remains less affected. Despite Am being a major α-decay source of high level waste generated from reprocessing, less information is available for Am bearing phases [18].

The aim of the present study is the investigation of the local environment of Am within the EFTTRA-T4 fuel after ~10 years of self-irradiation damage and following annealing by thermal treatment using EXAFS and comparing results with XRD characterization.

2. Experimental

To estimate the amount of macroscopic swelling, the dimensions (diameter, height) of the eight EFTTRA-T4 un-irradiated archive fuel pellets were measured with an optical device (Brown and Sharp Profile 20). The macroscopic swelling was then calculated by comparing them with the original pellet dimensions from the production in 1996. One pellet of the archive, aged EFTTRA-T4 fuel was selected for the investigations of the self-irradiation damage. The Am content of the pellet was 11.5 wt%, as determined by calorimetry in August 2005. This pellet was crushed and the X-ray powder pattern recorded using a Siemens D500 diffractometer operating with CuKα radiation. The 2θ scanning range was from 20° to 120°, with a 0.02° step size. In 1996, the X-ray pattern of the fresh fuel was measured with a Seifert MZ VI diffractometer, also operating with CuKα radiation. An annealed sample was prepared by sintering an aged pellet at 1873 K for 6 h in an Ar–H_2 (8% H_2) gas stream, the same thermal treatment conditions used for the fuel production in 1996.

2.1. Extended X-ray absorption fine structure (EXAFS)

For EXAFS measurement, 60 mg of both the aged and annealed sample powder were fixed in a steel shielded plexiglass cuvette and sealed with polyethylene foil. The annealed sample EXAFS was measured seven days after sintering. The EXAFS spectra of the Am L_3-edge were recorded at the INE-Beamline at the Ångströmquelle Karlsruhe, ANKA [19]. In addition, the Np L_3-edge X-ray absorption near edge structure (XANES) was recorded for both samples. The INE-Beamline optics includes a Ge(4 2 2) double-crystal monochromator (DCM) and two Rh coated mirrors for focusing and rejection of higher harmonics. The photon energy of the light coming off the DCM is calibrated against the first derivative XANES spectrum of a Zr foil, defined as 17 998 eV. All measurements were performed in transmission mode at room temperature.

The EXAFS oscillations were extracted according to standard procedures (background removal by polynomial pre-edge fit, normalization, cubic

spline fit) using the EXAFSPAK program suite [20]. The threshold energy of the Am L_3-edge, E_0, was set to 18 520 eV. Since only the lattice parameters, but not the atomic positions, are reported for $AmAlO_3$ [10], a spherical 8 Å cluster of atoms with Cartesian coordinates of the rhombohedral $NdAlO_3$ structure [13] and with Nd replaced by Am was used for the calculation of theoretical phase shifts, $\delta(k)$, and backscattering amplitudes, $F(k)$, (FEFF8 [21]). Both $NdAlO_3$ and $AmAlO_3$ have the same space group $R\bar{3}c$ with nearly identical lattice parameters, reflecting their similar ionic radii [22]. The amplitude reduction factor was held constant at 1.0 for the EXAFS fits. The shift in threshold energy, ΔE_0, was varied as a global parameter in the fit procedure.

3. Results

After 10 years of storage, the EFTTRA-T4 archive fuel pellets are intact but with visible cracks, mainly on the basal planes. As estimated by the change in pellet diameter and height, the macroscopic swelling $\Delta V/V_0$ of the fuel pellets since 1996 ranged from 4.9% to 8.0% with an average of 6.4%.

3.1. X-ray diffraction

The X-ray diffraction pattern of the aged EFTTRA-T4 fuel (measured in 2006) is shown in Fig. 1, together with the original pattern recorded just after fuel production in 1996. For comparison, reflexes for $AmAlO_3$ [23] are given in the bottom of the figure. The XRD pattern from 1996 reveals the presence of spinel ($a = 8.069$ Å) and of a second phase, whose peaks correspond to those of $AmAlO_3$ in the $R\bar{3}c$ space group [10,23]. Whereas the spinel peaks are relatively sharp (as can be seen from their $K\alpha_{1/2}$ splitting), the peaks of the second phase ($AmAlO_3$) are somewhat broader. This is likely caused by the rhombohedral distortion of the ideal perovskite structure resulting in a peak splitting. The quality of the data does not allow a detailed characterization of this phase, e.g., determination of lattice constants. The X-ray diffraction pattern recorded in 2006 also shows the peaks of the (inert) spinel matrix. However, peaks corresponding to the $AmAlO_3$ phase have completely disappeared. We attribute this to the amorphization/metamictization of the $AmAlO_3$ phase induced by 10 year self-irradiation damage. In contrast, the peaks of the spinel phase are remarkably sharp ($K\alpha_{1/2}$ splitting is also observed) and there is no indication of any peak broadening. No diffraction peaks corresponding MgO are present, a phase which might be formed in addition to $AmAlO_3$ through decomposition of $MgAl_2O_4$, indicating that the amount of MgO is below the detection limit of XRD or that MgO is dissolved in spinel [24].

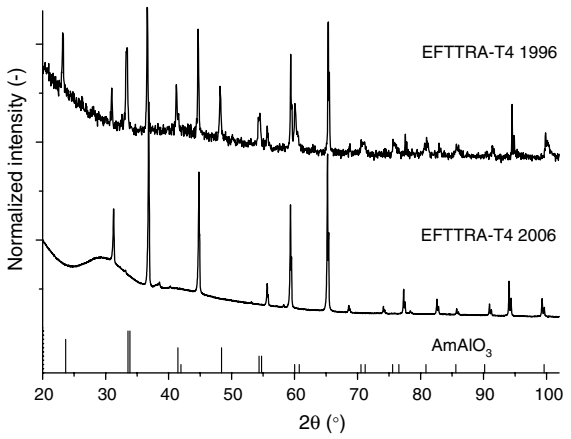

Fig. 1. X-ray diffraction pattern (CuKα) of EFTTRA-T4 fuel after preparation in 1996 (top) and in 2006 after 10 years storage (bottom). Positions of the rhombohedral $AmAlO_3$ [23] phase are also plotted for reference.

3.2. EXAFS results

Fig. 2 shows the k^3-weighted Am L_3-edge EXAFS spectra of the aged and annealed EFTTRA-T4 fuel and their corresponding Fourier transforms (FT). The EXAFS of the annealed sample is complex and numerous peaks are between 1.7 and 6.3 Å ($R + \Delta$) in the corresponding FT data. The second peak at 2.8 Å ($R + \Delta$) and third peak at 3.8 Å ($R + \Delta$), resulting from Am–Al and Am–Am scattering, are indicative of a perovskite-like $AmAlO_3$ structure. The first FT peak at 1.7 Å ($R + \Delta$) represents the first coordination shell with 12 oxygen atoms and has a lower intensity in the k^3-weighted data than the second peak, resulting from the second coordination shell of 8 Al atoms. A similar intensity trend was observed for $LaAlO_3$ in the $R\bar{3}c$ space group. The low first oxygen coordination shell intensity is due to a splitting of the Am–O distances. The oscillations of the three oxygen sub-shells comprising the first oxygen coordination shell are shifted in phase, due to their varying bond distances. This results in partial destructive interference and a reduction in overall intensity [25].

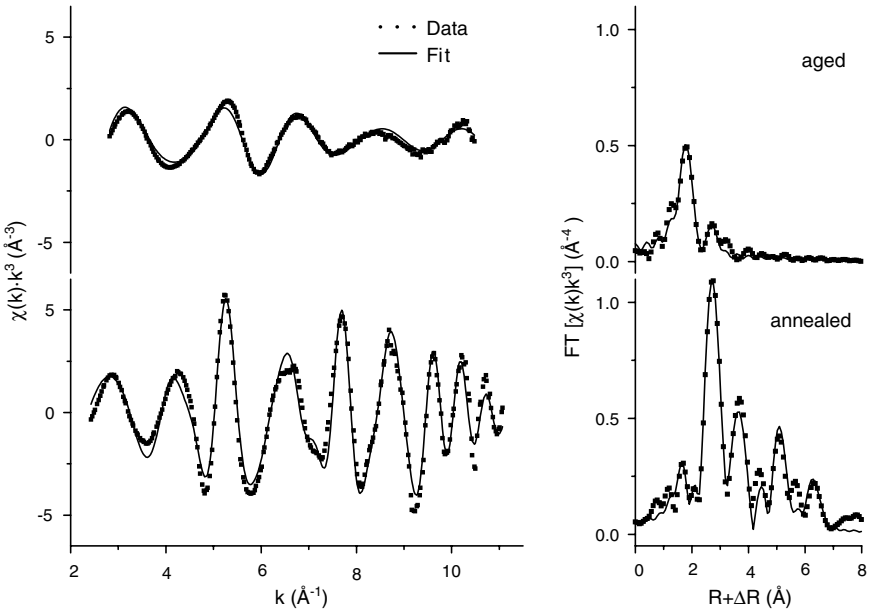

Fig. 2. Am L_3-edge EXAFS and corresponding Fourier transforms of aged and annealed EFTTRA-T4 fuel. Experimental data is shown as dots and best results of fits to the EXAFS equation as solid lines.

The oscillations in the EXAFS of the aged material is less complex than that for the annealed sample and is strongly dampened. In the FT, a broad peak at 1.9 Å ($R + \Delta$) and a second small peak at 2.8 Å ($R + \Delta$) are observed. The peak at 1.9 Å ($R + \Delta$) is approximately 40% more intense than that for the annealed material. This increase in intensity can be attributed to a smaller destructive interference of the Am–O distances. No further peaks are observed at higher radial distances. The radiation damage induced by α-decay of ^{241}Am removes the structural order from the second shell onward.

The Am L_3-edge EXAFS refinement of the annealed EFTTRA-T4 fuel was initiated in k-space using the coordination numbers (N) and interatomic distances (R) for the rhombohedral $NdAlO_3$ structure. N was held constant at the theoretical value for the $NdAlO_3$ structure during the fit. In this structure the first oxygen shell is split into three sub-shells at 2.44 Å (O_{1a}; $N = 3$), 2.66 Å (O_{1b}; $N = 6$), and 2.91 Å (O_{1c}; $N = 3$). Am–O distances and Debye–Waller factors, σ^2, for all these oxygen shells were included in the fit. Apart from the first Am shell (Am_1) at a distance of 3.75 Å, subsequent Al and Am shells (Al_1, Am_2, Al_2, and Am_3) should be distorted in the $R\bar{3}c$ structure. However, this static distortion does not exceed 0.05 Å so that these shells can be modelled by a single mean distance, just as for an ideal cubic perovskite structure. Evaluation of the FEFF8 generated backscattering paths calculated for $AmAlO_3$ (cf. Section 2) shows that, in addition to the single scattering (SS) paths, the 3-legged (MS3) and 4-legged (MS4) collinear multiple scattering (MS) paths are significant for the Am_2 (MS3: Am_0–O_1–Am_2–Am_0; MS4: Am_0–O_1–Am_2–O_1–Am_0) and Am_3 shells (MS3: Am_0–Al_1–Am_3–Am_0; MS4: Am_0–Al_1–Am_3–Al_1–Am_0). The EXAFS oscillations corresponding to the Am_2 and Am_3 shells are dominated by these collinear MS3 paths, whereas the contribution of the SS and MS4 paths are of minor importance. To reduce the number of free variable parameters in the fit, the distances and σ^2 for the MS paths were linked to those of their associated SS path. Results of fits to the aged archive and annealed samples are listed in Table 1.

As can be seen from Fig. 2 and Table 1, the experimental data of the annealed EFTTRA-T4 fuel is well-modelled with the $NdAlO_3$ structure, replacing Nd with Am. The distances of the three oxygen subshells determined by EXAFS analysis are shorter than those of the $NdAlO_3$ model compound. However, the determined Am–O distances are associated with a relatively large fit error (see Table 1). The strongest FT peak is caused by scattering on the 8 Al atoms at a mean distance of 3.25 ± 0.01 Å. A second Al shell (Al_2) with 24 Al atoms is expected near 6.26 Å. Since the contribution of this Al_2 shell is

Table 1
Structural parameters for Am in annealed and aged EFTTRA-T4 fuel[a]

Shell	N[b] (–)	R[c] (Å)	R (Å) $NdAlO_3$[d]	R (Å) $AmAlO_3$[e]	σ^2 (Å^2)[f]	ΔE_0 (eV)	Fit error[g]
Annealed EFTTRA-T4 fuel (crystalline $AmAlO_3$)							
O_{1a}	3	2.37 (1)	2.41	–	0.0061 (7)	3.1	0.302
O_{1b}	6	2.60 (1)	2.66	–	0.011 (1)		
O_{1c}	3	2.86 (1)	2.91	–	0.004 (1)		
Al_1	8	3.253 (3)	3.25 (1)	3.25 (2)	0.0054 (2)		
Am_1	6	3.753 (3)	3.75	3.76	0.0082 (3)		
Am_2	12	5.297 (4)	5.31 (2)	5.31 (2)	0.0098 (3)		
Am_3	8	6.500 (6)	6.50 (2)	6.51 (3)	0.0089 (5)		
Aged EFTTRA-T4 fuel (amorphous $AmAlO_3$) model A							
O_{1a}	3	2.36 (1)			0.0075 (5)	9.0	0.045
O_{1b}	6	2.58 (1)			0.023 (2)		
O_{1c}	3	2.88 (1)			0.011 (2)		
Al	1.1 (7)	3.28 (3)			0.02 (1)		
Aged EFTTRA-T4 fuel (amorphous $AmAlO_3$) model B							
O_1	3.5 (1)	2.34 (1)			0.0111 (5)	3.8	0.046
Al	2.8 (3)	3.18 (1)			0.017 (2)		

[a] Estimated standard deviations are given in parentheses.
[b] N, coordination number (held constant during the fit).
[c] R, radial distance determined in this study.
[d] Ref. [13].
[e] Ref. [10]. Atomic position of oxygen is not reported for $AmAlO_3$.
[f] σ^2, Debye–Waller factor.
[g] Residuals are given as the normalized fit error $\sum[\chi_{data}(k)\cdot k^3 - \chi_{fit}(k)\cdot k^3]^2/(P-F)$ (P number of data points, F number of variables).

low (3% of the total intensity), attempts to include it in the fits lead to large statistical errors. For these reasons this shell was excluded in the fit. Three Am shells are clearly distinguishable at high $R+\Delta$. The interatomic distance of the Am_1 shell is 3.75 ± 0.01 Å. Those for the more distant Am_2 and Am_3 shells are at 5.30 ± 0.01 Å and at 6.50 ± 0.01 Å, respectively. These values compare well with those reported in the literature [10,13].

The Am L_3-edge EXAFS of the aged EFTTRA-T4 fuel shows no peaks in the FT beyond 2.8 Å ($R+\Delta$). The EXAFS of this sample was fitted applying a model (A) based on the $NdAlO_3$ structure including the split oxygen shell O_{1a}, O_{1b}, O_{1c} and a single Al shell. N was held constant at the theoretical value for the $NdAlO_3$ structure during the fit for the oxygen atoms but allowed to vary for the Al shell. The distances obtained for the oxygen sub-shells of the first coordination sphere, as well as the distance of the Al shell, are similar to those of the crystalline material (Table 1). Approximately one Al atom at 3.28 ± 0.1 Å from the central Am atom is found. This is much lower than the expected $N = 8$ in the crystalline material. A fit with N(Al) held constant at 8 lead to unreasonably high σ^2 (cf. [26]). When N of the oxygen sub-shells was allowed to vary in the fit procedure, but their sum constrained to 12, similar bond lengths were obtained, and N was approximately 4 for all three sub-shells.

In addition, a simplified fit model (B) based on a single Am–O distance instead of three sub-shells was used to describe the Am L_3 EXAFS of the aged EFTTRA-T4 fuel. About 3–4 oxygen atoms were found at Am–O distances of 2.34 Å (Table 1). Both N(O) and R(O) in model B are too low compared with the mean distance in the crystalline material or in a relaxed (cubic) structural arrangement (i.e., 12 O at a mean distance of 2.65 Å). Furthermore, fitting the annealed sample's EXAFS with a single Am–O distance gives similar results incompatible with the crystal structure. Since structure determination of disordered materials (rhombohedral distortion, amorphization) is generally difficult, model A is a rational compromise between spectroscopy and chemistry.

3.3. Np and Am L_3-edge XANES

During the 10 years storage of the un-irradiated EFTTRA-T4 pellets, 1.4% of the initial ^{241}Am decayed to ^{237}Np. The L_3-edge XANES of Np and Am are shown in Fig. 3 for the aged and annealed material. There is no significant shift in the Np and Am L_3-edge energy comparing the aged and

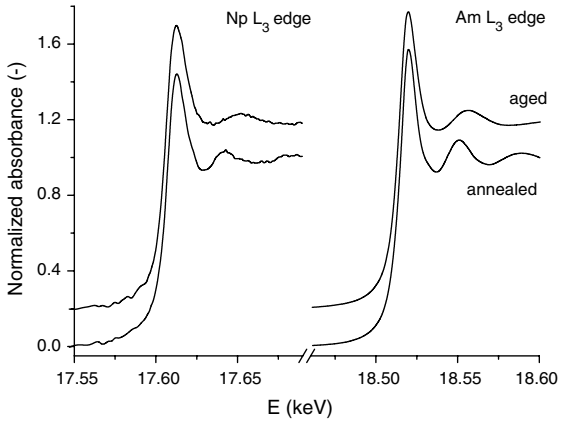

Fig. 3. Np and Am L_3-edge XANES of the aged (top) and annealed (bottom) EFTTRA-T4 fuel.

annealing sample. Since the annealing was performed under reducing conditions (Ar/H_2 gas stream at 1873 K), the actinides are predominantly present as Am^{3+} and Np^{4+} both in the aged and annealed material. The post-edge region of the XANES, which reflects more the local atomic structure around Np and Am than their electronic states, is different for the aged (amorphous) and annealed (crystalline) sample. However, the post-edge region is quite similar for Np and Am within the same sample (aged/annealed) indicating similar local coordination environments for Am and its daughter Np both in the aged and annealed sample.

4. Discussion

The Am L_3-edge EXAFS of the annealed EFTTRA-T4 fuel is well-described by the rhombohedral $AmAlO_3$ ($NdAlO_3$) structure. Typical features of this structure are the distorted first oxygen shell and aluminium and americium shells at higher distances. The more distorted orthorhombic structure of $SmAlO_3$ also exhibits a strongly split first aluminium shell [12], which was not observed in the annealed EFTTRA-T4 fuel.

The α-particles emitted from ^{241}Am release their energy by ionization processes over 10–20 μm, causing atomic displacements primarily near the end of the alpha particle path. The much slower but heavier alpha recoil nuclei loose their energy in a range of 30–40 nm, producing 1000–2000 atomic displacements per decay [6]. Since the Am in the EFTTRA-T4 fuel is located in volumes less than 3 μm in diameter, the radiation damage in $AmAlO_3$ is mainly caused by displacements due to the recoil nuclei and the damage in the spinel matrix is mainly affected by the α-particles. Minor effects are due to α-particles reaching surrounding $AmAlO_3$ grains and also due to recoil nuclei reaching the spinel matrix in direct contact with the $AmAlO_3$ phase.

The oxygen shell around the Am atoms in the EFTTRA-T4 fuel exhibits a similar structure in both the annealed and aged material. The three oxygen sub-shell contributions to the EXAFS partially cancel each other out, resulting in a broad FT peak with low intensity. As indicated from X-ray diffraction investigations on $^{244}CmAlO_3$, the rhombohedral material becomes cubic upon self-irradiation before total amorphization occurs [11]. In a cubic perovskite structure the first oxygen coordination shell does not exhibit static disorder. The aged $AmAlO_3$ in the archive fuel pellet, however, shows no indication of a single oxygen coordination shell at about 2.65 Å. Rather, the EXAFS indicate a distribution of the oxygen atoms around the central Am atom, similar to those in the annealed material. Apart from the distorted oxygen shell, a shell with approximately one Al atom is observed at an interatomic Am–Al distance of 3.28 Å in the aged material. The reduction of the Al coordination number from eight in the annealed material to ~1 in the aged fuel suggests that the structural disorder of the Al shell is severe. It appears that in the radiation damaged $AmAlO_3$ the Am–O near-neighbour structure with three oxygen sub-shells remains. In contrast, it appears that the Al shell exhibits a highly variable configuration, which leads to the extreme loss in EXAFS amplitude observed for this shell.

The radiation damage certainly depends on the distance from the atom that decays. The X-ray diffraction results for $CmAlO_3$ indicate a local increase in symmetry prior to amorphization [11]. A similar effect was found for the first oxygen shell in zircon doped with ^{238}Pu [17]. In contrast, the more distant shells in zircon are not perturbed significantly by α-decay damage. Damage is material dependent and the extent to which a material is damage resistant is believed to be related to the covalent component in the bonding of the material [27]. Molecular dynamics simulations of the decay and damage processes in this material could help to elucidate the exact mechanisms. Such calculations should be coupled to experimental investigations (XRD, EXAFS) and extended to the characterization of the recovery (even stepwise) of the material crystal structure by means of thermal treatment.

The X-ray diffraction pattern of the aged EFTTRA-T4 fuel shows crystalline peaks of the spinel

matrix; no peak broadening was observed. This reflects the amorphization resistance of $MgAl_2O_4$ against α-particles-one of the reasons why spinel was chosen as inert matrix for the EFTTRA-T4 experiment. Recognizing that the $AmAlO_3$ is dispersed in the spinel matrix, the spinel directly surrounding the 2–3 μm $AmAlO_3$ grains should be more affected by the α-particles from the ^{241}Am decay than the more distant inner regions of the spinel grains. The latter then exhibit a coherent diffraction pattern, whereas the part of the spinel in close contact with $AmAlO_3$ could be nearly amorphous. Further investigations using high temperature X-ray diffraction and electron microscopy are underway to identify this possible structural alterations and their recovery.

5. Conclusion

Within the EFTTRA-T4 project a $MgAl_2O_4$ based inert matrix fuel for ^{241}Am transmutation was produced in 1996. Am L_3-edge EXAFS of the annealed material indicate that Am is present as $AmAlO_3$. During 10 years of storage the archive material accumulated self-irradiation α-damage of $4.3 \times 10^{18}\ g^{-1}$ fuel. The archive material displays no $AmAlO_3$ diffraction pattern, indicating amorphization of the aged material by the corresponding cumulative α-decays of $2.9 \times 10^{19}\ g^{-1}$ in the $AmAlO_3$ phase. The Am L_3-edge EXAFS of the amorphous $AmAlO_3$ shows that structural order is limited to the first oxygen shell around Am. The rhombohedral splitting of the Am–O shell into three sub-shells prevails. In contrast, approximately one near-neighbour Al atom at a Am–Al distance of 3.28 Å is found. The extreme loss in oscillatory amplitude indicates a highly variable configuration in the Am–Al shell structure. Further investigations are underway to understand the process of damage formation in the material. In particular thermal annealing will be used to induce re-crystallization in the material. Should the recovery occur in a stepwise or shell-wise fashion, indications of the structure of the damaged material can be determined. MD simulations of the damage and recovery processes are also under consideration.

Acknowledgements

We would like to acknowledge the assistance of D. Bouexiere for performing X-ray diffraction measurement, J. Rothe for assistance using the INE-Beamline, and ANKA for providing beamtime for the EXAFS measurements.

References

[1] C. Degueldre, J.M. Paratte, J. Nucl. Mater. 274 (1999) 1.
[2] K. Richter, A. Fernez, J. Somers, J. Nucl. Mater. 249 (1997) 121.
[3] R.J.M. Konings, R. Conrad, G. Dassel, B.J. Pijlgroms, J. Somers, E. Toscano, J. Nucl. Mater. 282 (2000) 159.
[4] F.C. Klaasen, K. Bakker, R.P.C. Schram, R. Klein Meulekamp, R. Conrad, J. Somers, R.J.M. Konings, J. Nucl. Mater. 319 (2003) 108.
[5] T. Wiss, R.J.M. Konings, C.T. Walker, H. Thiele, J. Nucl. Mater. 320 (2003) 85.
[6] W.J. Weber, R.C. Ewing, C.R.A. Catlow, T. Diaz de la Rubia T, L.W. Hobbs, C. Kinoshita, Hj. Matzke, A.T. Motta, M. Natasi, E.K.H. Salje, E.R. Vance, S.J. Zinkle, J. Mater. Res. 13 (1998) 1434.
[7] S. Geller, V.B. Bala, Acta Cryst. 9 (1956) 1019.
[8] P.D. Dernier, R.G. Maines, Mater. Res. Bull. 6 (1971) 433.
[9] L.E. Russel, J.D.L. Harrison, N.H. Brett, J. Nucl. Mater. 2 (1960) 310.
[10] C. Keller, K.H. Walter, J. Inorg. Nucl. Chem. 27 (1965) 1247.
[11] W.C. Mosley, J. Am. Ceram. Soc. 54 (1971) 475.
[12] M. Marezio, P.D. Dernier, J.P. Remeika, J. Solid State Chem. 4 (1972) 11.
[13] C.J. Howard, B.J. Kennedy, B.C. Chakoumakos, J. Phys.: Condens. Matter 12 (2000) 349.
[14] R.C. Ewing, W.J. Weber, F.W. Clinard Jr., Prog. Nucl. Energy 29 (1995) 63.
[15] R.C. Ewing, B.C. Chakoumakos, G.L. Lumpkin, T. Murakami, R.B. Greegor, F.W. Lytle, Nucl. Instrum. and Meth. B 32 (1988) 487.
[16] R.B. Greegor, F.W. Lytle, R.J. Livak, F.W. Clinard Jr., J. Nucl. Mater. 152 (1988) 270.
[17] N.J. Hess, W.J. Weber, S.D. Conradson, J. Alloys Compd. 271–273 (1998) 240.
[18] F. Goubard, P. Griesmar, A. Tabuteau, J. Solid State Chem. 178 (2005) 1898.
[19] M.A. Denecke, J. Rothe, K. Dardenne, H. Blank, J. Hormes, Phys. Scr. T115 (2005) 1001.
[20] G.N. George, I.J. Pickering, EXAFSPAK: A suite of computer programs for analysis of X-ray absorption spectra, Stanford Synchrotron Radiation Laboratory, Stanford, 1995.
[21] A.L. Ankudinov, B. Ravel, J.J. Rehr, S.D. Conradson, Phys. Rev. B 58 (1998) 7565.
[22] F. David, J. Less-Common Met. 121 (1986) 27.
[23] K.H. Walter, Ternäre Oxide des drei- bis sechswertigen Americiums, Kernforschungszentrum Karlsruhe, KFK 280, 1965.
[24] B. Hallstedt, J. Am. Ceram. Soc. 75 (1992) 1497.
[25] F. Deganello, A. Longo, A. Martorana, J. Solid State Chem. 175 (2003) 289.
[26] B.K. Teo, EXAFS: Basic Principles Data Analysis, Springer-Verlag, Berlin, 1986.
[27] K. Trachenko, M. Pruneda, E. Artacho, T. Dove, Phys. Rev. B 70 (2004) 134112.